# *The Calibration and Description of a Wind-Tunnel for Studying Stratified Flows*

Technical Report EM-71-2

WALTER R. DEBLER
RICHARD D. MONTGOMERY



December 1971

Office of Naval Research
Contract N00014-67-A-0181-0008

Department of Engineering Mechanics
Fluid Mechanics Section

THE UNIVERSITY OF MICHIGAN
COLLEGE OF ENGINEERING
Department of Engineering Mechanics
Fluid Mechanics Section

Technical Report EM-71-2

# THE CALIBRATION AND DESCRIPTION OF A WIND-TUNNEL FOR STUDYING STRATIFIED FLOWS

Walter R. Debler
Richard D. Montgomery

ORA Project 013660 with the
Office of Naval Research
Contract N00014-67-A-0181-0008

Under the Direction of

James W. Daily

Walter Debler

administrated through:

OFFICE OF RESEARCH ADMINISTRATION ANN ARBOR, MICHIGAN

December 1971

TABLE OF CONTENTS

## LIST OF ILLUSTRATIONS

## ABSTRACT

A wind-tunnel is described in which the air temperature can be varied in the vertical direction. The facility is used to study stratified flows. The velocity and temperature characteristics of the wind-tunnel were determined through a series of calibration tests. The results are presented herein. The performance of the wind tunnel is considered to satisfactory for its intend purpose.

## 1. Wind Tunnel Description

The wind tunnel, which is described in this report, is shown schematically in figure 1. Here one sees an open-loop wind tunnel with a contraction ratio of 13/1. After the air has passed through the contraction, it is heated as it continues through by some stainless-steel, honey-comb strips. Each strip has its own source of electrical energy. This is supplied by a set of A. C. welding transformers. The test section, two feet high and four feet wide, is thirty feet long. The aluminum roof of the first segment can be heated by thermostat controlled, infra-red heating elements. This was done to preserve the temperature profile at the upper boundary. Similarly, cooling water can be circulated through the rectangular aluminum conduits which support the floor. The heated air leaves the wind tunnel through a diffuser section with an inner body to guide the flow past an axial flow fan. This unit has an attachment with which one can adjust the angle of attack of the blades. At the exit of the fan a trumpet-shaped diffuser directs the flow radially. It passes through a series of cooling coils which are intended to bring the air back to room temperature. The laboratory in which the wind tunnel stands is sufficiently large (104 by 176 feet) and until now it has not been necessary to use these coolers. The motor which drives the fan has a rated horsepower of 7.5; the speed is controlled by an eddy-current coupling. This motor-control assembly will provide for air speeds in the test section of approximately 40 feet per second.

The details of the wind tunnel can be seen in figure 2 through 10. Figure 2 shows wind tunnel entrance (thirteen feet wide by eight feet high). Some nylon mosquito netting is visible in the picture over the entrance to the inlet section. There is actually two sections of netting between which there is a sheet of polyurethane foam that was donated by the Scott Paper Company. This serves to filter the air and the netting supports it from behind and prevents accidental damage

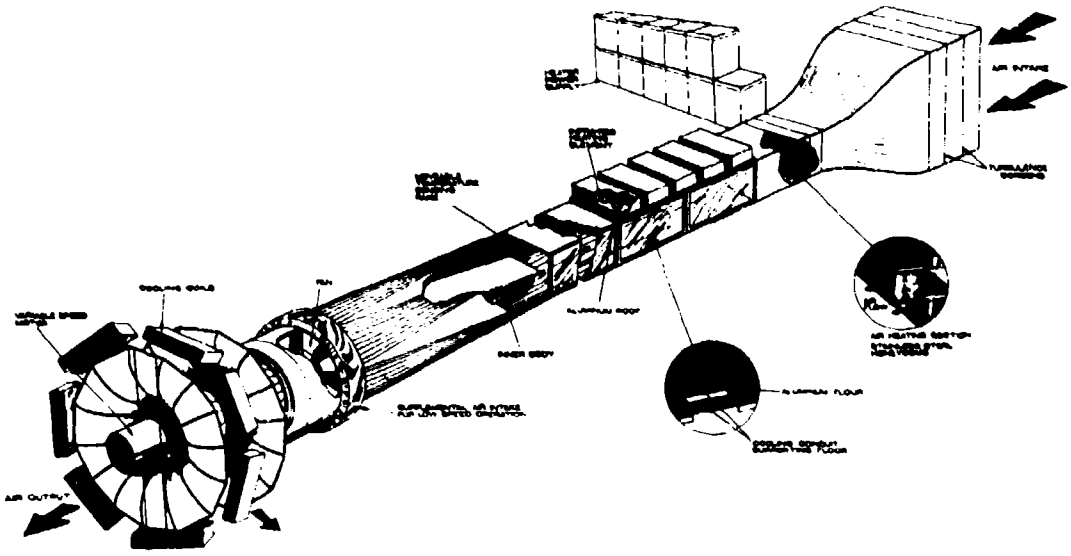

Fig. 1. Pictorial view of wind tunnel

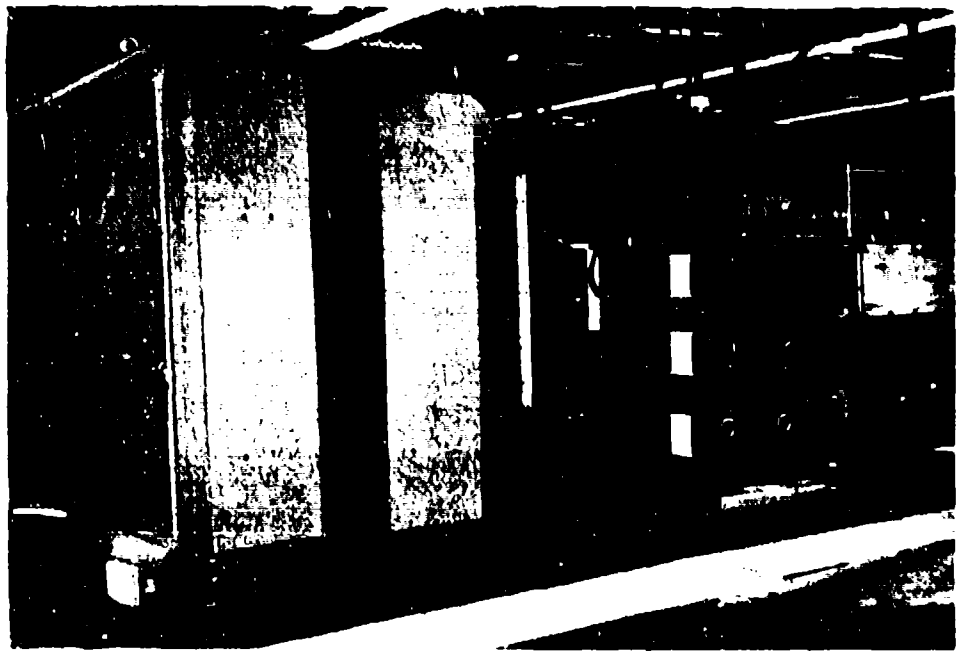

Fig. 2. Entrance, stilling and contraction sections. Six of the eleven welding transformers are also shown.

to the foam in the front. Behind this inlet filter there is a section of four inch deep aluminum honey-comb. The core of the honey-comb is three-fourths of an inch. The settling chamber is built in three parts. The first and last parts provide a thirteen by eight foot frame over which is stretched stainless steel screen, four in total, in order to improve the settling chamber's effectiveness. Figure 2 also shows the six, 300 ampere (100 per cent duty cycle) welding transformer which provide the current to the second, third, fourth, fifth, sixth and seventh lowest heating strips in the tunnel. The lowest strip is not heated. The remaining strips are heated with 500 ampere welders. These cannot be seen in any of the figures. One can barely observe some wheels in the upper left hand corner of the figure. These are part of two floor model fans that were mounted on top of the tunnel and which were directed in front of the tunnel's inlet to improve the temperature homogenity of the incoming air. At the far right of the figure the vertical section of polyethylene sheeting can be seen. This serves to incapsulate the first ten feet of the test section and thereby minimize the air leakage. The many parts associated with heating the roof of the first section resulted in a number of joints that permitted air to be sucked into the tunnel.

The contraction section needs no further comment. However, the tunnel's heat section will be described in some detail. The stainless-steel honey-comb that was used was forty-eight inches long, two inches high and two inches deep (i.e. in the direction of the core). A segment of the length of one of these heating sections is shown in the top of figure 3. The core size is a nominal one-quarter inch. These stainless-steel sections were mounted in two vertical planes. Each of these two sections had a space of two inches between each of the honey-comb strips. They were installed in each of the sections so that a honey-comb strip in one section was at the same horizontal level as a space in the second heater section and vice versa. The nature of this construction can be

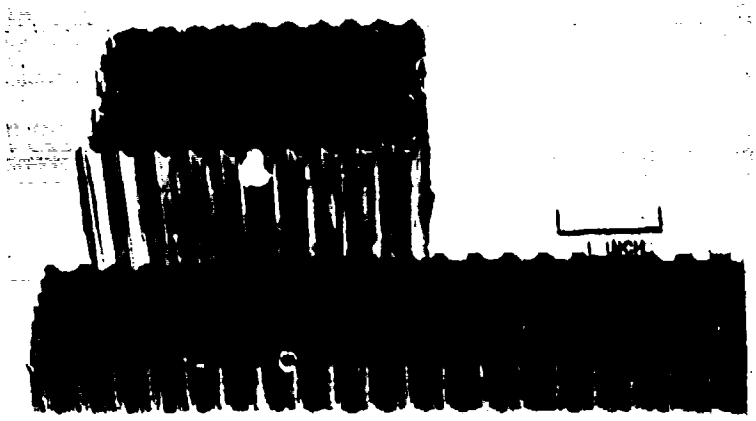

Fig. 3. Honeycomb used in heater section. Upper, is stainless steel for the heating elements. Lower, is phenolic material used to guide the air between two successive heater stages (c.f. insert to fig. 1.).

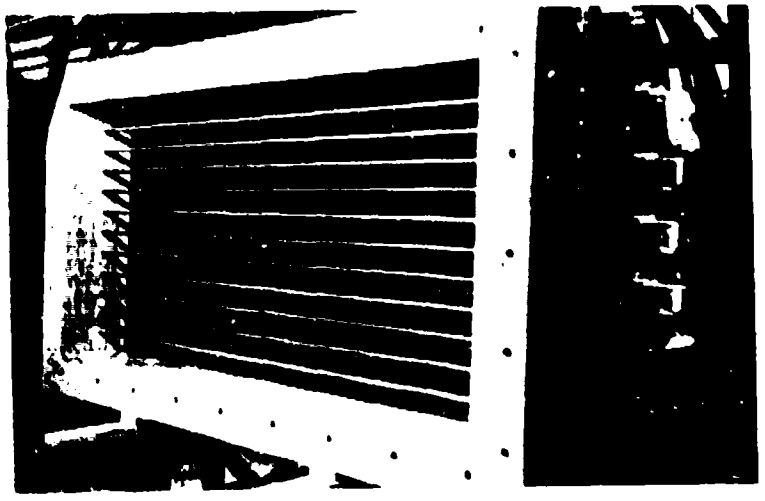

Fig. 4. Heater section showing method of support of elements by tension strips that are insulated from heating elements by glass tubing. One half inch brass rods to promote interfacial mixing can be seen.

seen in the insert figure 1. The two inch vertical space between each heating element provides for electrical insolation but yet made the heater appear without gaps when viewed in the direction of the tunnel axis. Originally a one-half inch air gap (in the direction of the tunnel's axis) separated the two segments of the heater. The first detailed results of the vertical temperature profile in the test sectio indicated that some of the air might be going over and under some of the heating strips and thereby caused some unwanted charges in the temperature gradient. A piece of one-half inch thick fiberglass honey-comb was inserted as a divider in the vertical air gap between the two heating sections. This eliminated any possibility of the air moving along a path of low resistance, and consequently low heat transfer, by avoiding the heating element. This fiberglass honey-comb is illustrated in the lower half of figure 3 prior to installation. Its thermal characteristics were tested by trying, in vain, to ignite or melt the plastic with the flame from a match.

Figure 4 shows the heater assembly. At the right is a series of welding lug connectors which are attached to some one-half inch diameter threaded brass rods which are not visible in the photograph. These rods in turn are threaded into two inch cubes of copper that are brazed to the ends of the stainless steel segments. On the threaded rods are nuts which can be tightened and thereby pre-tension the stainless-steel sections. However, this action did not eliminate all of the undesirable sag in the four foot span. The solution to this problem is shown in figure 4. It consists of a strip of stainless steel that is inserted in the air gap between the successive honey-comb heaters. This strip has a series of "Y-shaped" fingers spot welded to it. In the trough of each Y section a piece of heat resistance glass tubing was placed. The tubing was wired to the Y section to secure it and a separate wire through the glass tubing that restrained the heating element. The glass tubing was necessary to provide electrical installation. The photograph shows eleven one-half inch place rods that

are situated downstream of the heater so that their centers correspond to the elevations of the tops and bottoms of the various honey-comb strips. Since each of the honey-comb would be heated separately it was expected that the temperature profile of the air leaving the heater would have a "staircase" distribution. It was intended that these rods would provide some interfacial mixing and to improve the linearity of the temperature profile. Results that were obtained with this heater configuration will be presented shortly.

Figure 5 shows the last ten foot segment of the test section with its oak frame construction and plexiglass windows. Beyond that there is a diffuser, motor, and exit section with the attached coolers. These coolers and the drive motor can also be seen in figure 6. The exit diffuser was made from thin fiberglass sheeting that was pre-cut according to some developed pattern, fastened to a light weight medal frame and then the seams were bounded with fiberglass cloth strips and a readily available boat-patching kit.

Some of the mechanical devices that were developed to aid in the recording of the temperature and velocity of the air stream are shown in the following four figures. Figure 7 shows a platform which rests upon the wind tunnel flow and which can be propelled over a distance of ten feet by means of the two rectangular rods which connect it to the drive mechanism at the terminus test section. One of these rectangular rods can be seen at the bottom left of the photograph. Attached to its side is a ten foot length of rack that is engaged by a drive pinion at the rear of the test section. The two pinions (one for each rectangular rod) are driven by a reversible drill motor, the speed of which is admusted by a transformer. Naturally, a speed reducer has been incorporated into the gear train. Suitable intermediate connecting links can be used so as to position the instrument platform in various places in the tunnel. With these links in place, ten feet of adjustment is again possible.

Fig. 5. Side view of third, 10 foot test section, diffusor and exit.

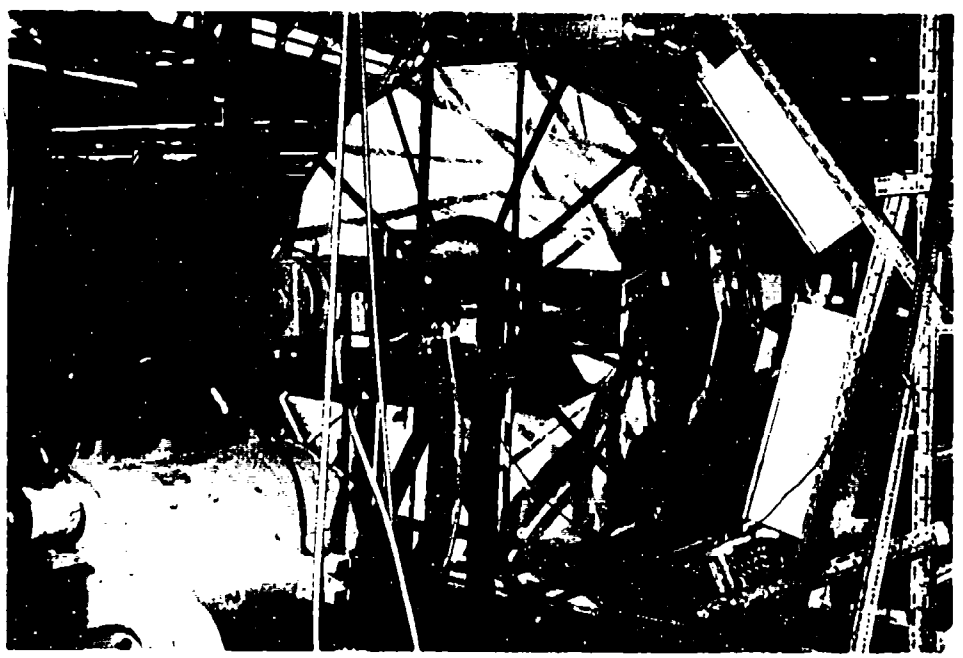

Fig. 6. Wind tunnel exit and drive.

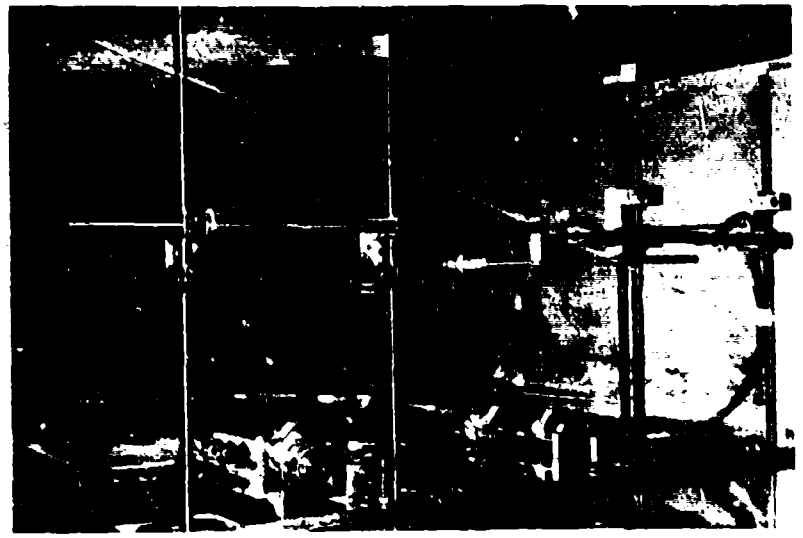

Fig. 7. Probe manipulator. The two inner, vertical rods support the vertical drive mechanism.

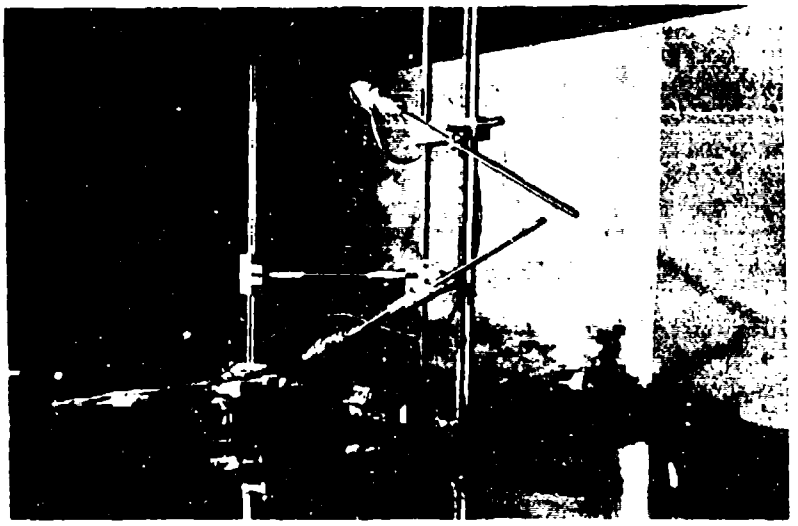

Fig. 8. Probe manipulator for performing horizontal and vertical correlations. Rear vertical rod is stationary. Forward vertical rod can move laterally on threaded rod. Position is indicated by counter. Entire unit can be translated along tunnel's floor

The platform contains two vertical drive screws that move two horizontal bars up and down. One can mount his instrumentation on these bars. A hot wire anemometer and pitot-static are shown in the illustration. The elevation of the horizontal bars is determined by the counter at the top of the drive screws. These are rotated through a gear train driven by selsen motors which are elctrically connected to matching units outside the wind tunnel. The ability to adjust the probes from outside the tunnel was on the one hand a great convenience but on the other hand almost a necessity because it was not deamed wise to open the tunnel while operating and thereby destroy the temperature gradient that had been established. Some overheating and possible damage to the heater may also have ensued. Figure 8 shows another probe adjusting mechanism. This was built in order to be able to move one probe laterally and vertically with respect to another which is at a fixed location. Again, counters were used to determine the position. This carriage assembly could also be moved along the tunnel access by the rack and pinion arrangement that was described previously.

In order to specify the temperature gradient within the tunnel prior to the air passing through a biplanar grid or past an object the sensor shown in figure 9 was constructed. It consists of a series of copper-constanant thermocouples which are supported by hypodermic needles. Thermocouples are on one inch centers and after a desired temperature gradient has been established the entire thermocouple rake can be retracted into the tunnel's side wall. The recesses for the vertical member and hypodermic needles are visible in the photo-graph. Also to be seen is a piece of shadowgraph quality glass that was installed as part of an optical system for the tunnel. In figure 10 one sees a view along the side of the tunnel which was not open to

Fig. 9. Temperature rake for sensing the undisturbed temperature distribution. Rake retracts into wall. Shadowgraph window also is visible.

Fig. 10. View of support for temperature rate (at center of picture) showing guide channel and reference ice-bath. Cement block column supports channel in which a guide block slides. The guide block contains the thermocouple terminal strip and a guide pin to assure the position of the thermocouple rake when retracting it into the recesses in the sidewall of the wind tunnel. Covered mirror for shadowgraph visible on second, block column.

viewing. It is presented to show the three brick columns. The one on the right supports a parabolic mirror with its dusk cover. The light source for this optical system is located on the brick column in the very left and is occluded by the stack of welders. The center column serves as a support for a piece of aluminum channel which guides the temperature rake when inserting it into the air stream and withdrawing it into the wall. A hole and tapered pin assembly are part of the light color object over the center column and align the rake properly so that none of the thermocouples is damaged when retracting the assembly into the side wall of the tunnel. The cold junction for the thermocouples is also to be seen next to this aluminum channel. Only copper conductors must go from this temperature rake to the recording instrument.

## 2. The Velocity and Temperature Calibration

A series of studies were planned at a wind speed of twenty feet per second (6.1m/sec.). In order to assure the two-dimensionality of the flow and preservation of its characteristics at various down-stream stations, a lengthy series of tests were conducted. The probe manipulator shown in figure 7 was used to transport a one-eight inch diameter pitot-static tube which itself had been individually calibrated, for determining the velocity field. The pressure difference was recorded on a micromanometer. An oil at specific gravity of 1.0 was used in this device. The gauge which measured the displacement of the incline leg of the manometer had divisions of 0.0001 inches. The position of the needle was interpolated between these divisions. A thermocouple recorded the temperature of the fluid in the manometer well. A determination of the specific gravity-temperature characteristics of the fluid was performed so that these temperature data could be included in a computational program for specifying the field velocity. Figure 11 shows the vertical profile of the wind speed taken at two positions along the wind tunnel axis. All of the dimensions (i.e. longitudinal, x; vertical, y; and lateral, z) have been non-dimensionalized with the distance M which corresponded to the mesh width of a bi-planar grid that was subsequently employed. M was two inches for this grid which had, incidently, one-quarter inch stainless steel, polished rods as its elements. Figure 11 shows that the velocities have been non-dimensionalized; $\bar{U}_c$ is the center-line velocity. No vertical temperature gradient had been applied to the air stream for the data shown. The position x = 0 designates the plane in which it was intended to mount the grid, circular cylinder or other test objects. The conclusion can be drawn from the figure that for $\frac{y}{M}$ between 8 and 16 the velocity is constant and for $\frac{y}{M}$

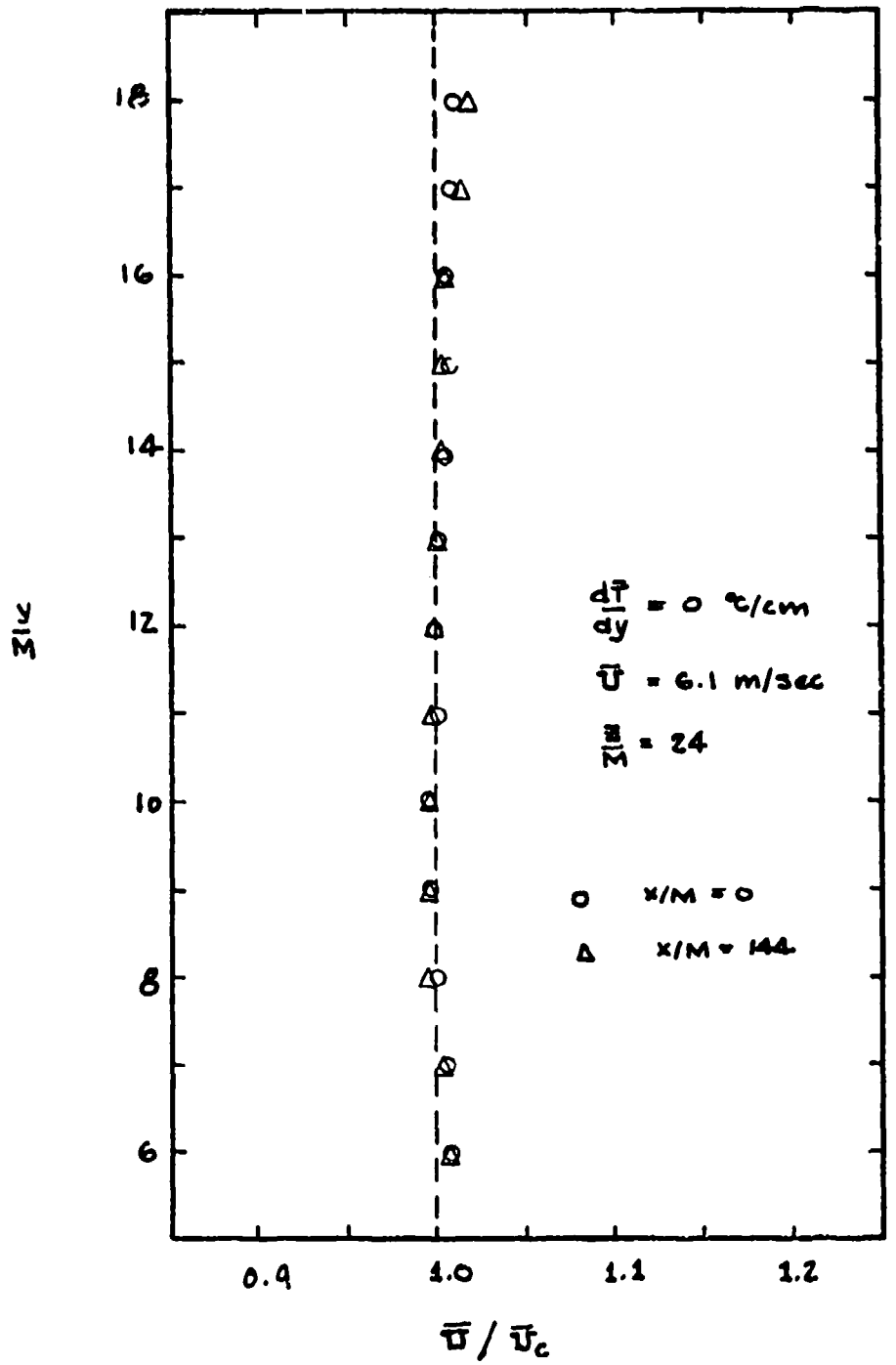


Fig. 11. Vertical mean velocity distribution.

between 6 and 18 it is within 99 per cent of the center-line value, even at $\frac{x}{M}$ of 144. It should be noted that these data were taken $\frac{z}{M} = 24$, the center-plane of the tunnel. One should remark here that the wind tunnel's speed was set by referring to a retractable pitot-tube that was about one meter ahead of the test station, $x = 0$. It was determined before hand what the pressure difference of this pitot-tube must have in order that the speed by 6.1m/sec. at the test station.

The lateral or span-wise velocity distribution was checked by measuring with a series of 12 hypodermic needles arranged in a rake-line array and read, one by one, with the micromanometer. See figure 12. A number of tests conducted previously had shown that there was no systematic error in this rake. The only measurements shown in figure 13 are taken at the mid-height of the tunnel and at two stations along its axis. Again no temperature gradient was applied to the air.

The speed control would sometimes not keep the fan turning at the desired setting. Rather, the speed would wander, slightly, above and below the prescribed setting. This may have been due to the characteristics of the unit or to the fluctuations in the electric power that was supplied. The speed of the drive motor was monitored by placing a 120-tooth gear on the drive shaft and recording the fluctuations, produced by a magnetic sensor, with a digital electronic counter. With a nominal count of 1500/second, a variation of $\pm 25$ counts/second was sometimes observed. If the speed proved to be very erratic, tests in which a great deal of confidence was placed were not continued. In most of the data which follows the points represent information that was taken at or very near a prescribed motor speed setting. If the speed wandered slightly from the prescribed value, the observer waited until it returned to the proper value and then recorded his observations. Often this resulted in

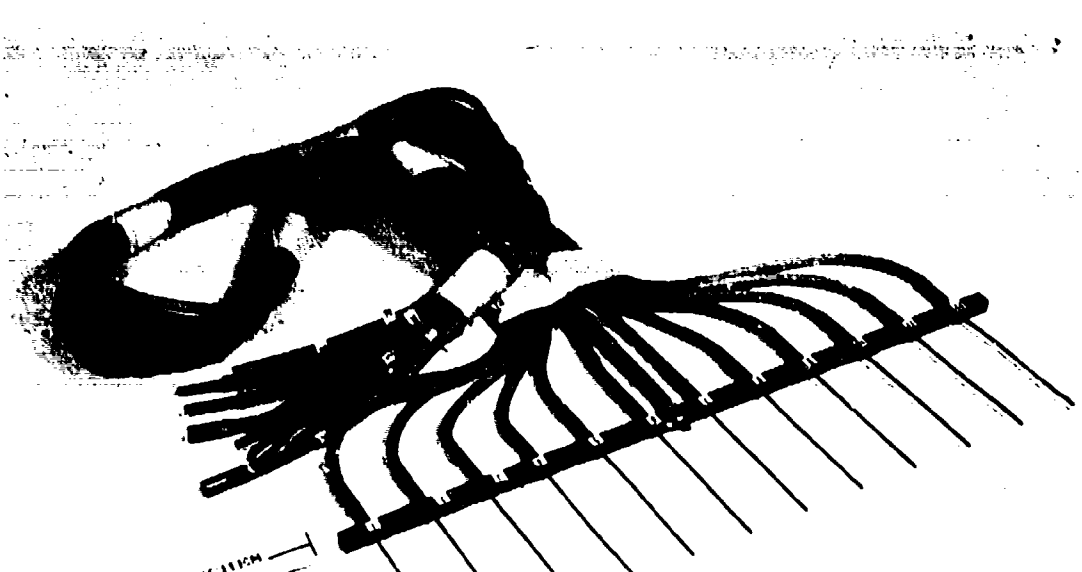

Fig. 12. Impact tube rake for measuring the free-stream velocity distribution in the wind tunnel.

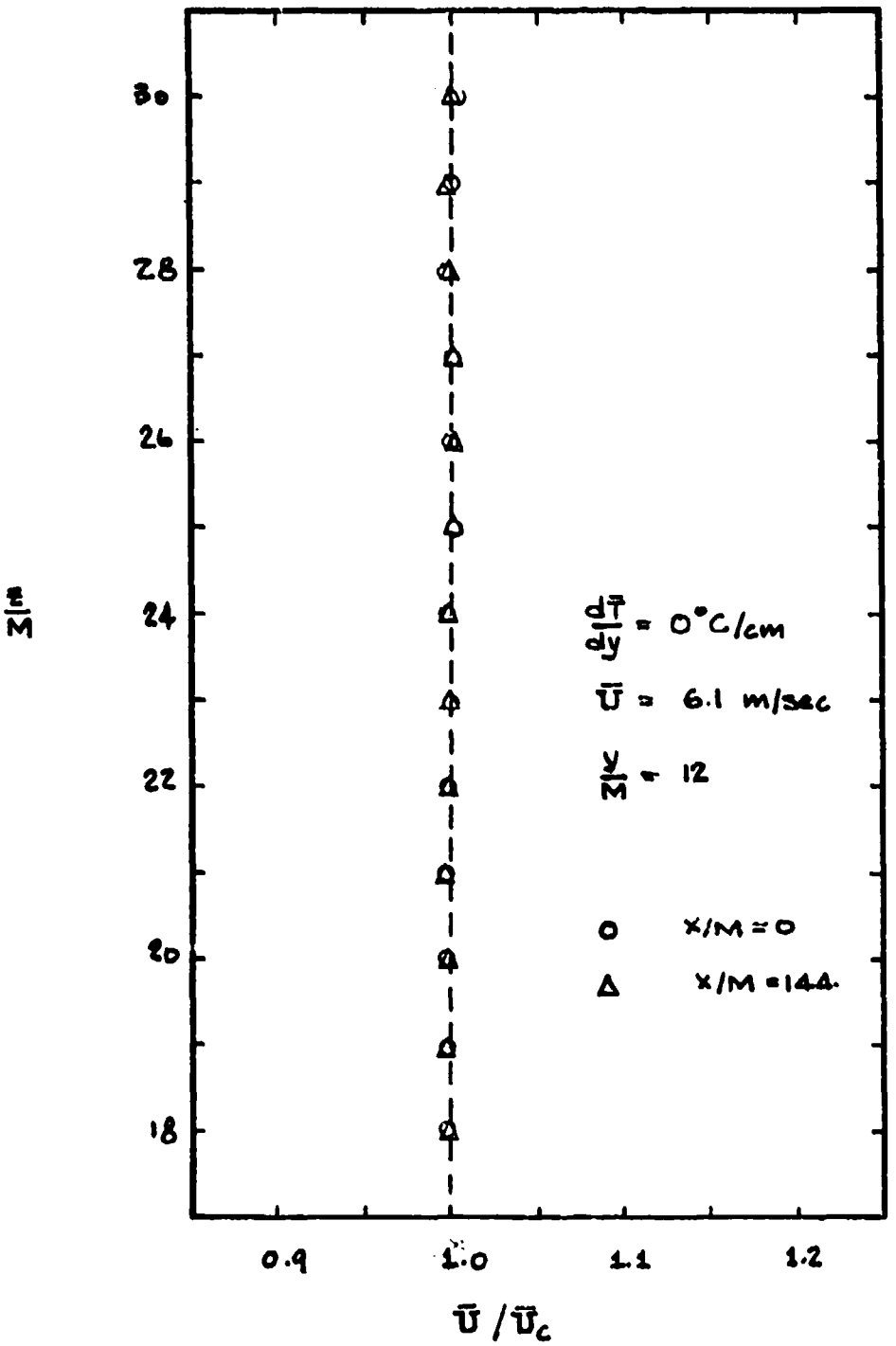


Fig. 13. Lateral (or horizontal) mean velocity distribution.

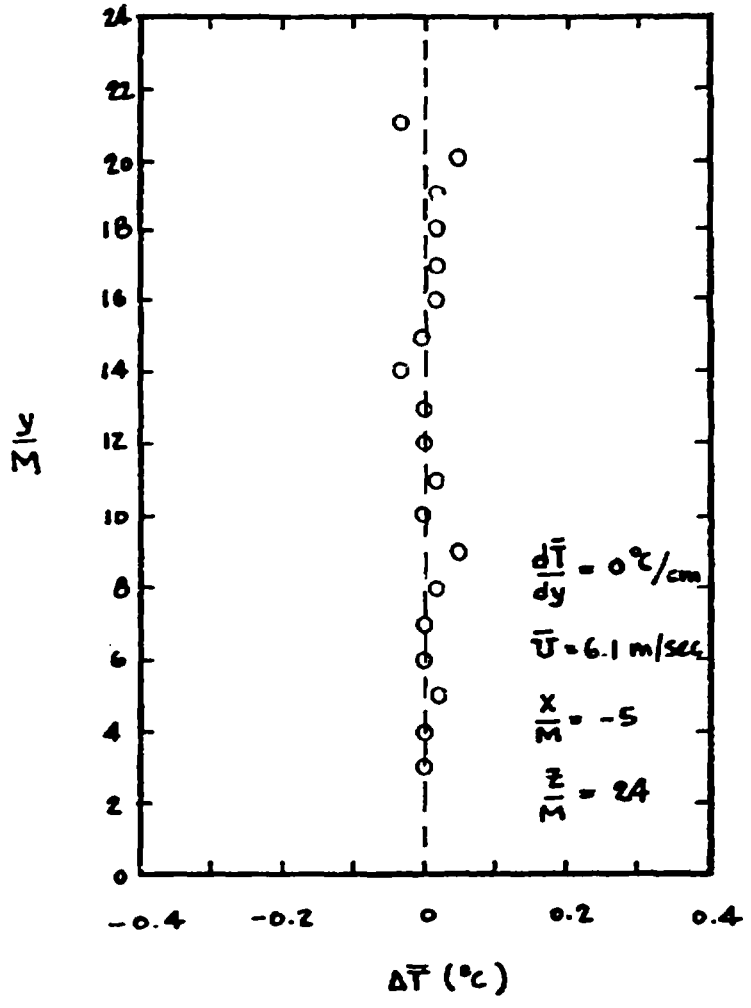


Fig. 14 a. Vertical mean temperature distribution

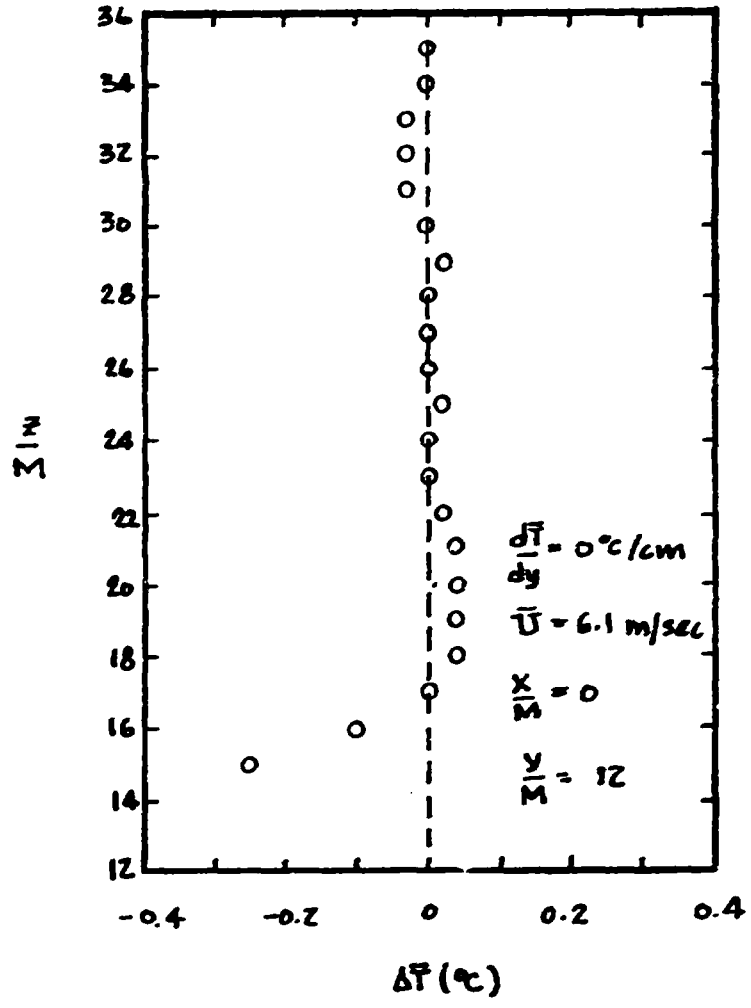


Fig. 14 b. Lateral mean temperature distribution (Z increases away from viewing windows - cf, Figure 5)

tests being twice as long as what might be expected.

In figure 14 one sees the variation of temperatures both vertically and laterally in the tunnel without any heat being applied to the air. The $\Delta \bar{t}$ represents the temperature difference from that at midheight and center plane for the two stations shown. The temperatures were sensed with copper-contanant thermocouples (36 gauge wire diameter) and recorded with a digital voltmeter. The wind tunnel tended to suck in warm air from the ceiling of the laboratory and, in the winter, cold air from the floor. In order to prevent the latter from being too prevalent, one of the entrances of the laboratory near the wind tunnel was sealed off with plywood and masking tape. The fans, shown in figure 2, were used to promote a uniform temperature in the wind tunnel's entrance. A typical calibration for the thermocouples is shown in figure 15. All the thermocouples used were made from the same reel of duplex wire and the individual performance was not calibrated, but was referred to calibrations similar to that shown in figure 15.

The current settings on the welders which supplied the energy to the heating strips were found by previous tests and could be set to give an approximation to the desired temperature gradient. Subsequent measurements by a thermocouple rake, (cf. figure 9) were used to readjust the current settings to get the desired linearity of the temperature distribution. Figure 16 presents such distributions. In making temperature measurements, smaller intervals than shown in figure 16 were taken at first to assure that there were no local discontinuities in the gradient. Experiments with the heater used in these tests showed that the measurements on one inch intervals could be relied upon to establish a linear temperature profile. Figure 17 shows that a desired temperature gradient once established is convected along the tunnel in a very satisfactory

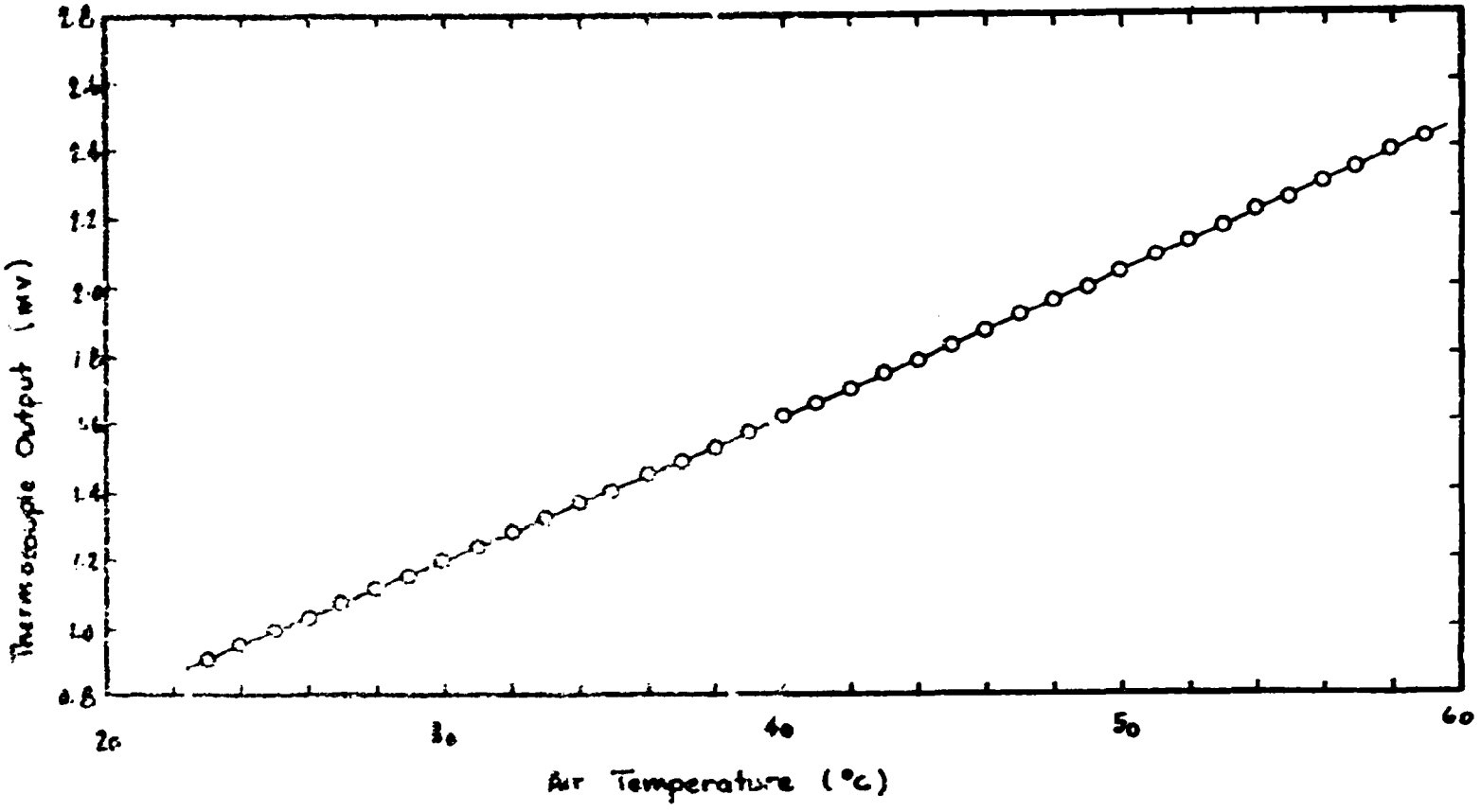


Fig. 13. Typical calibration curve for copper - constantan thermocouple

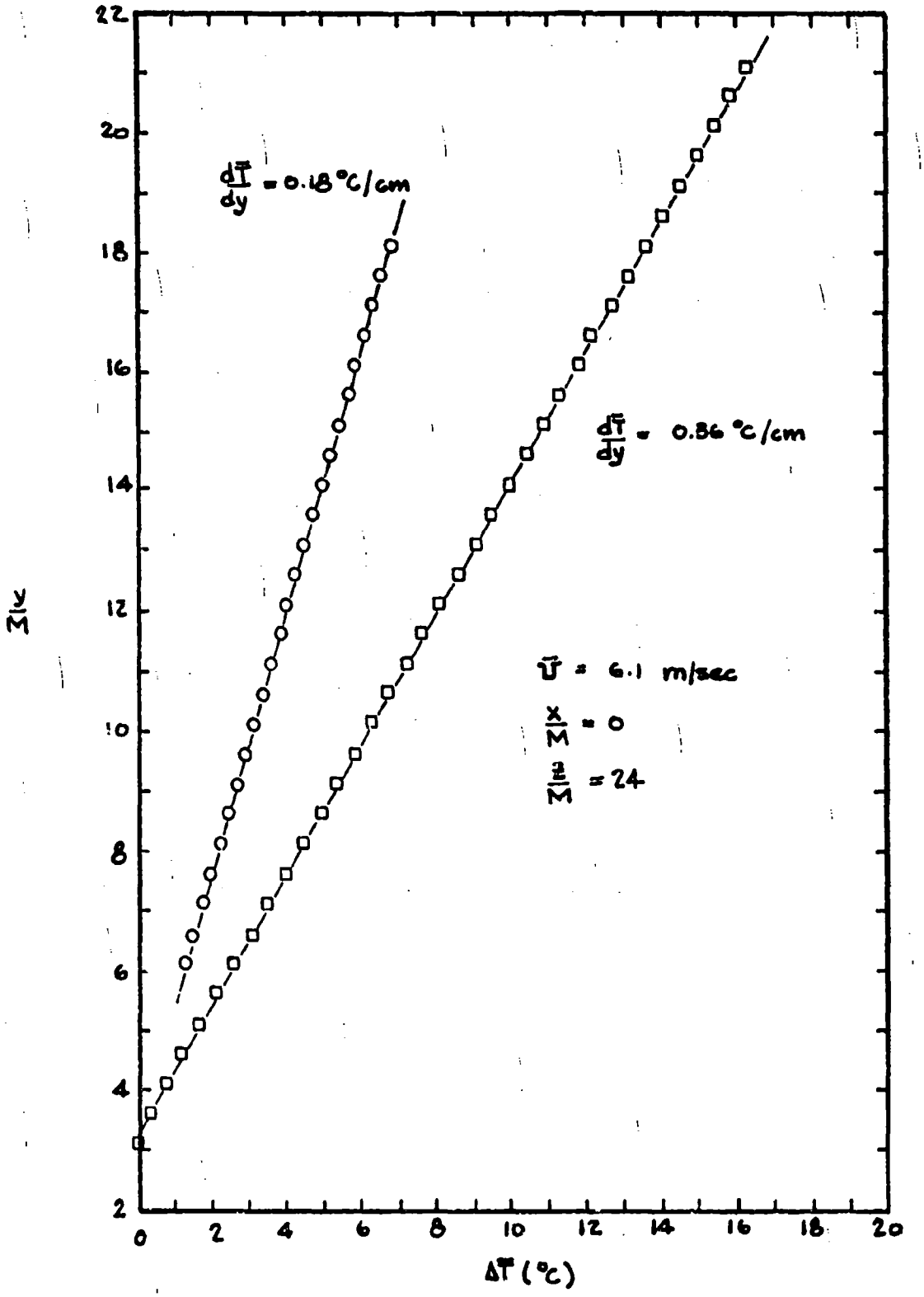


Fig. 16. Typical vertical mean temperature distributions

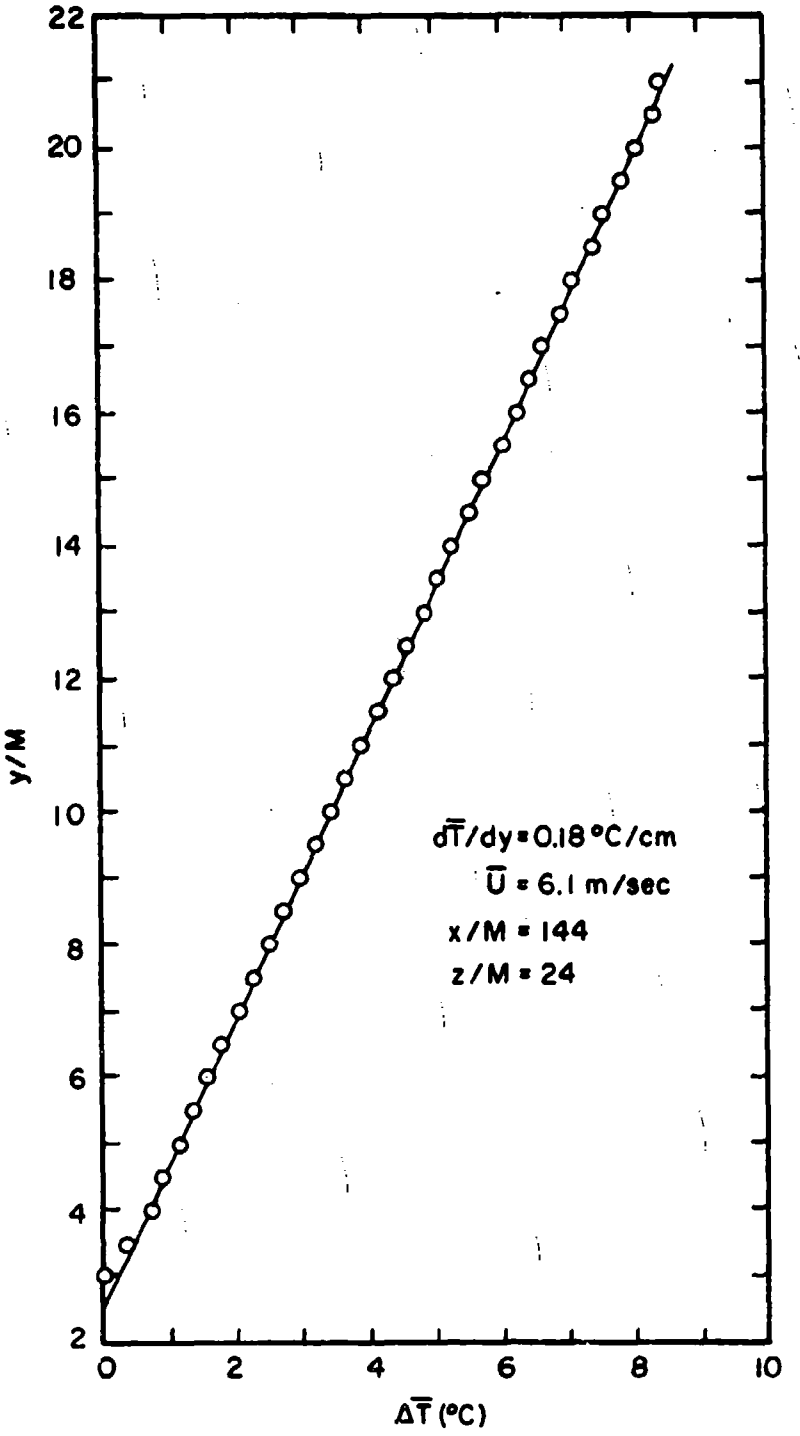


Fig. 17. Vertical mean temperature gradient at x/M = 144 (No Grid)

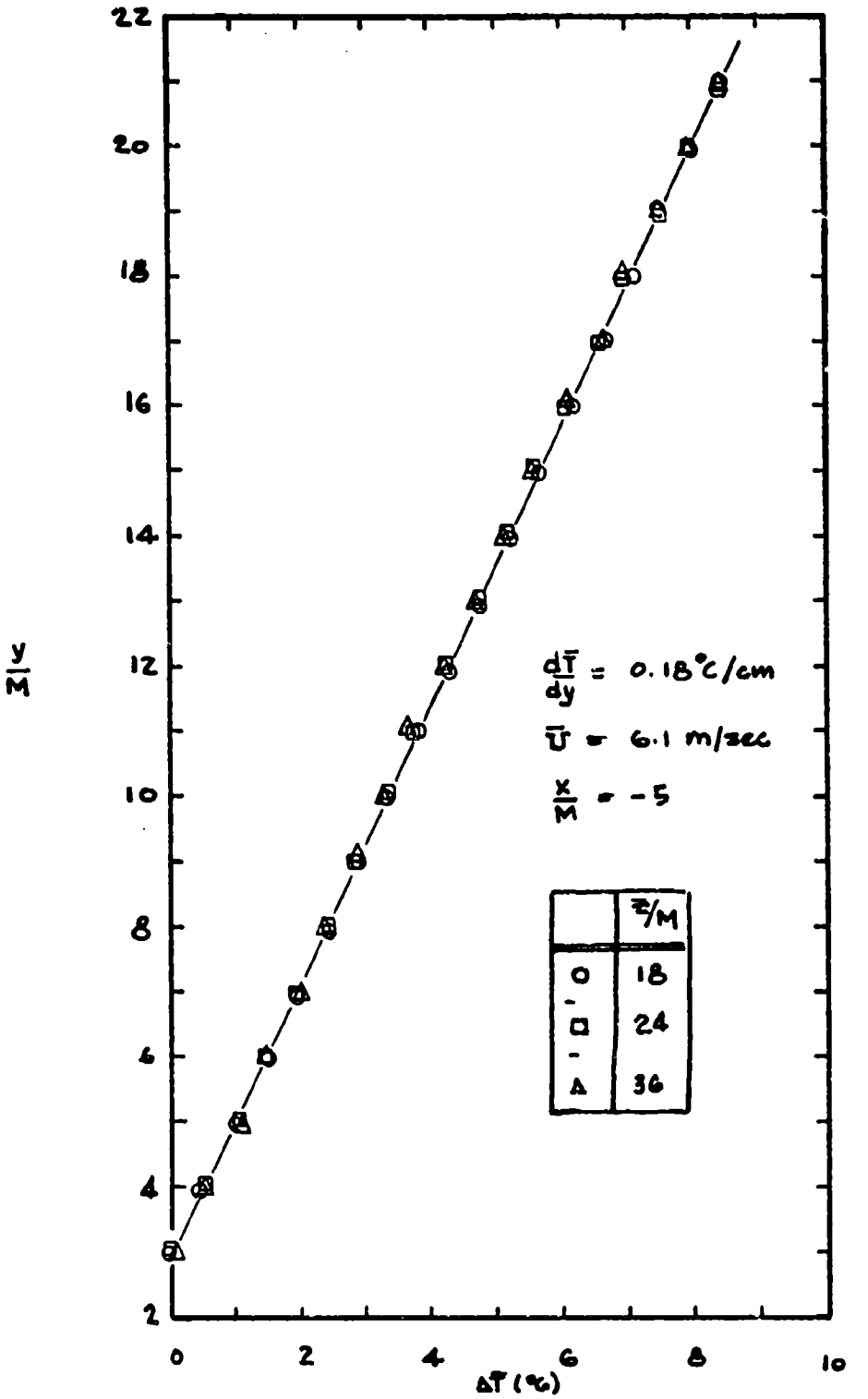


Fig. 18. Two - dimensionality of vertical mean temperature distribution

way.

The span-wise uniformity of temperature gradient is suggested in figure 18. Here the temperature gradient is measured at three lateral stations in the tunnel. Tests were made of the temperature profile nearer the side walls, e.g. $\frac{z}{M}$ of 6, 12, and 42, and they showed no significant deviation from the data shown in the last figure.

The experiments that are anticipated in this stratified wind tunnel often would require a great deal of time to complete. Consequently there was a desire to learn whether or not the temperature gradient, once set, would drift from the prescribed value. To test this possibility two "standard", gradients were established and readings were taken over four hour periods. The results are shown in figures 19 and 20. They show that the gradients can be set and readings can be taken subsequently with confidence. It should be noted that the data in figure 19 were compiled after normal working hours. This was the case for most of the tests with the wind tunnel in order to minimize the temperature disturbances in the laboratory due to the many people opening and closing doors.

Because the heater is in the flow path and the heating process could produce an effective resistance to the flow, a test was made to find the effect of the temperature gradient on the velocity profile. Figure 21 shows that at $x = 0$, and on the tunnel's center plane, there was virtually no effect upon the vertical velocity profile by introducing a temperature gradient. Equally well, the span-wise velocity distribution does not appear to be influenced by the action of the heater. This can be seen in figure 22.

Turbulence intensity in the tunnel when no structures are in the flow was tested at an air speed of 6.1m/sec. A DISA constant-

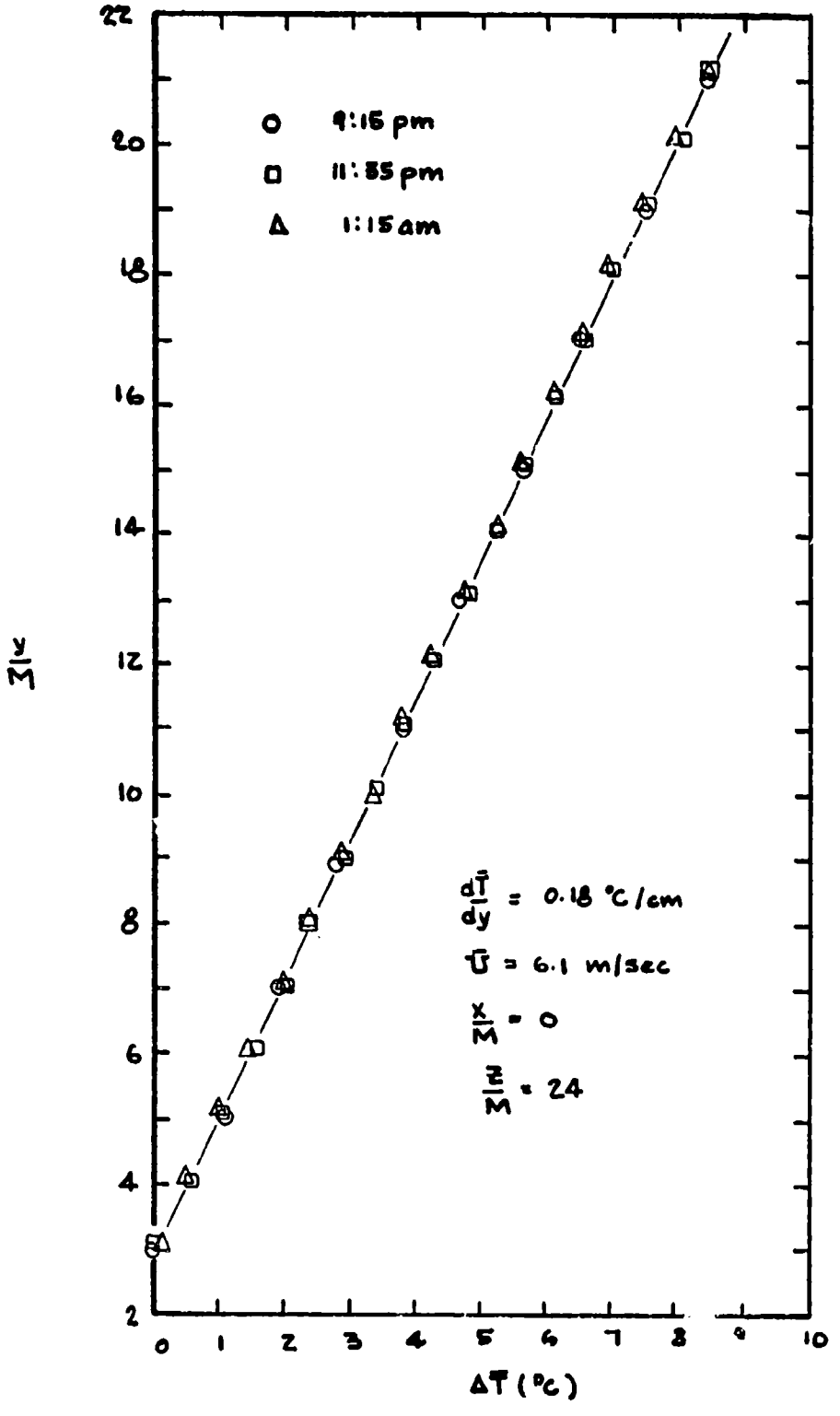


Fig. 19. Steadiness of vertical mean temperature distribution $d\bar{T}/dy$ = 0.18 °C/cm)

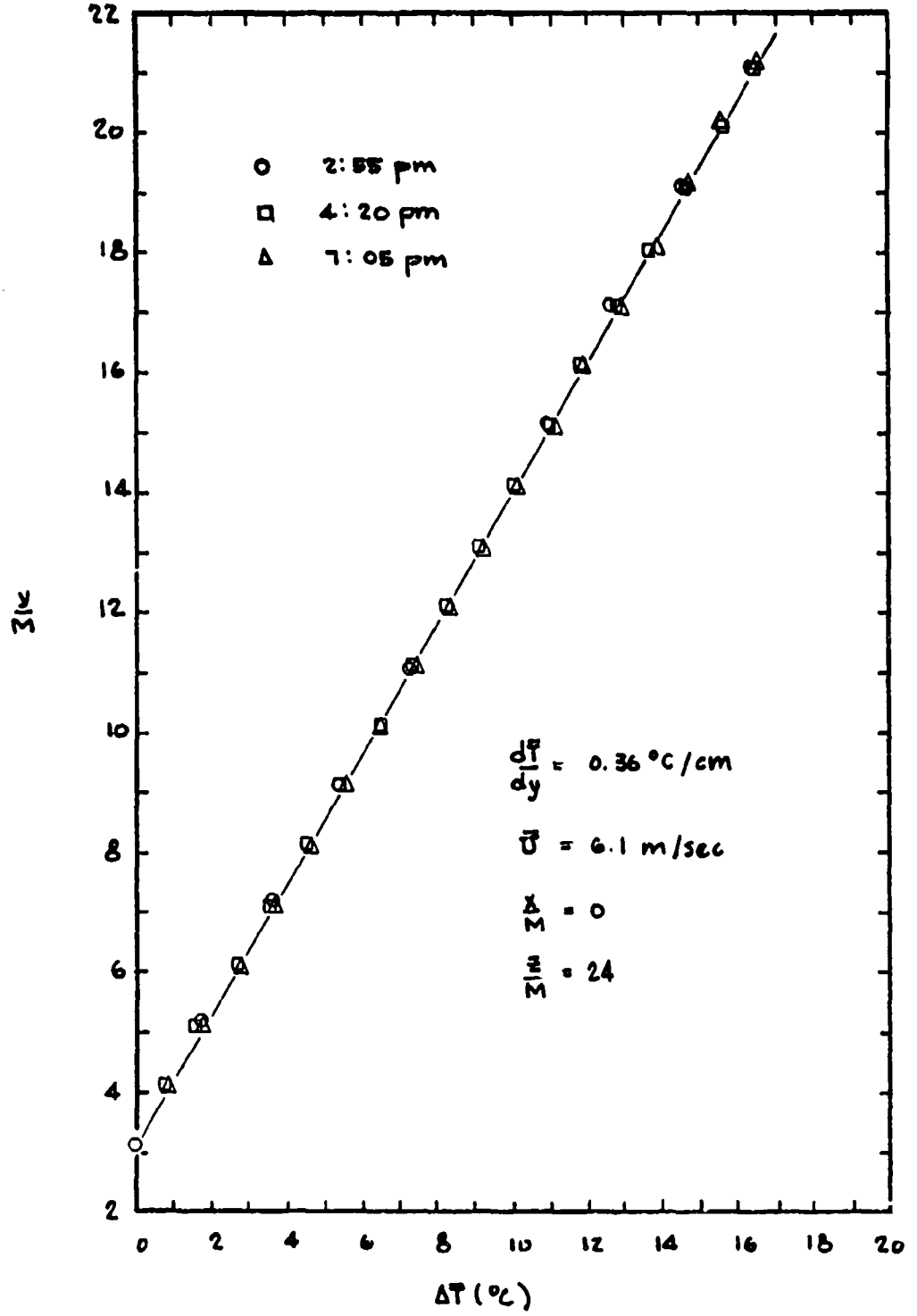


Fig. 20. Steadiness of vertical mean temperature distribution ($d\bar{T}/dy$ = 0.36 °C/cm)

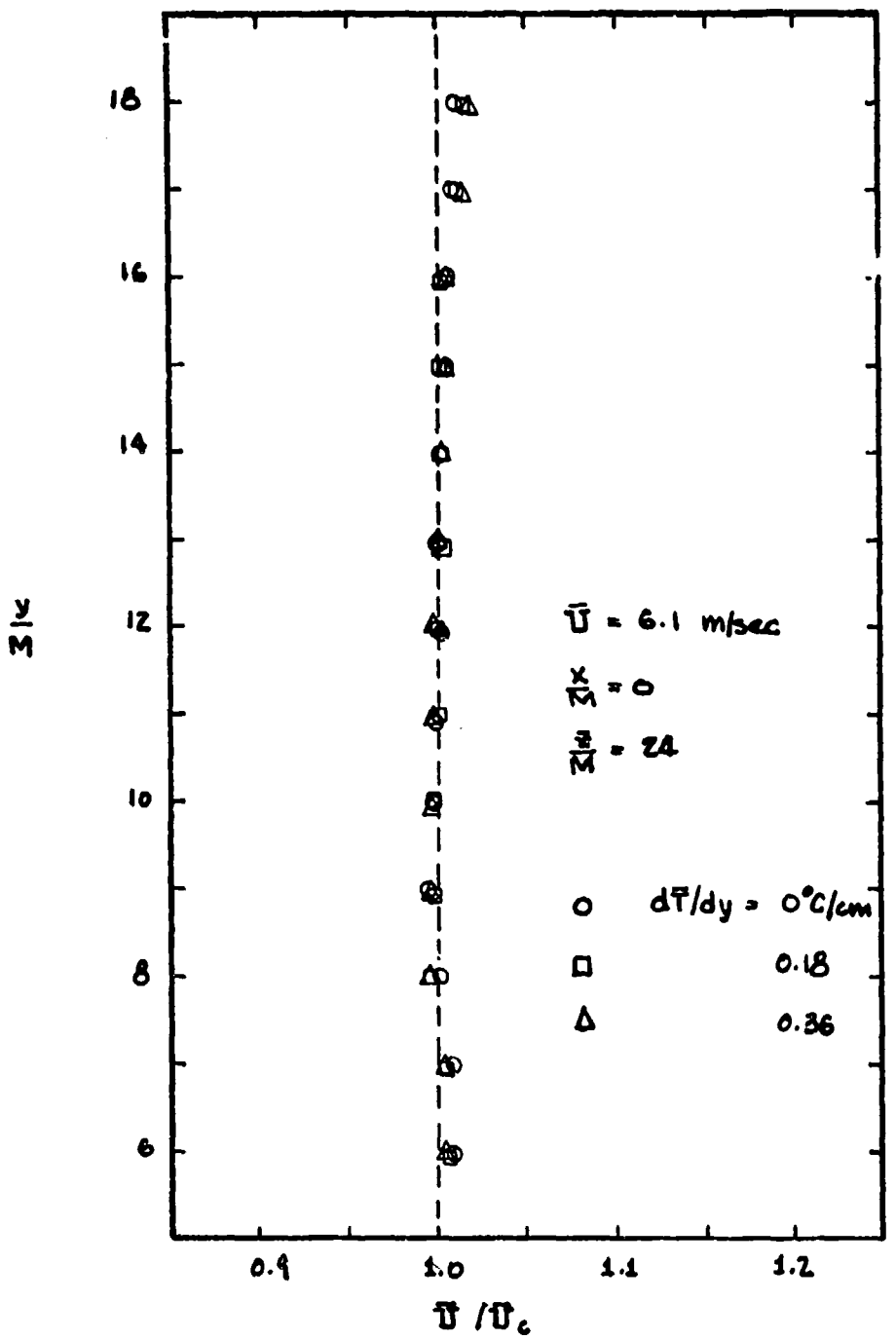


Fig. 21. Temperature effect upon mean vertical velocity distribution

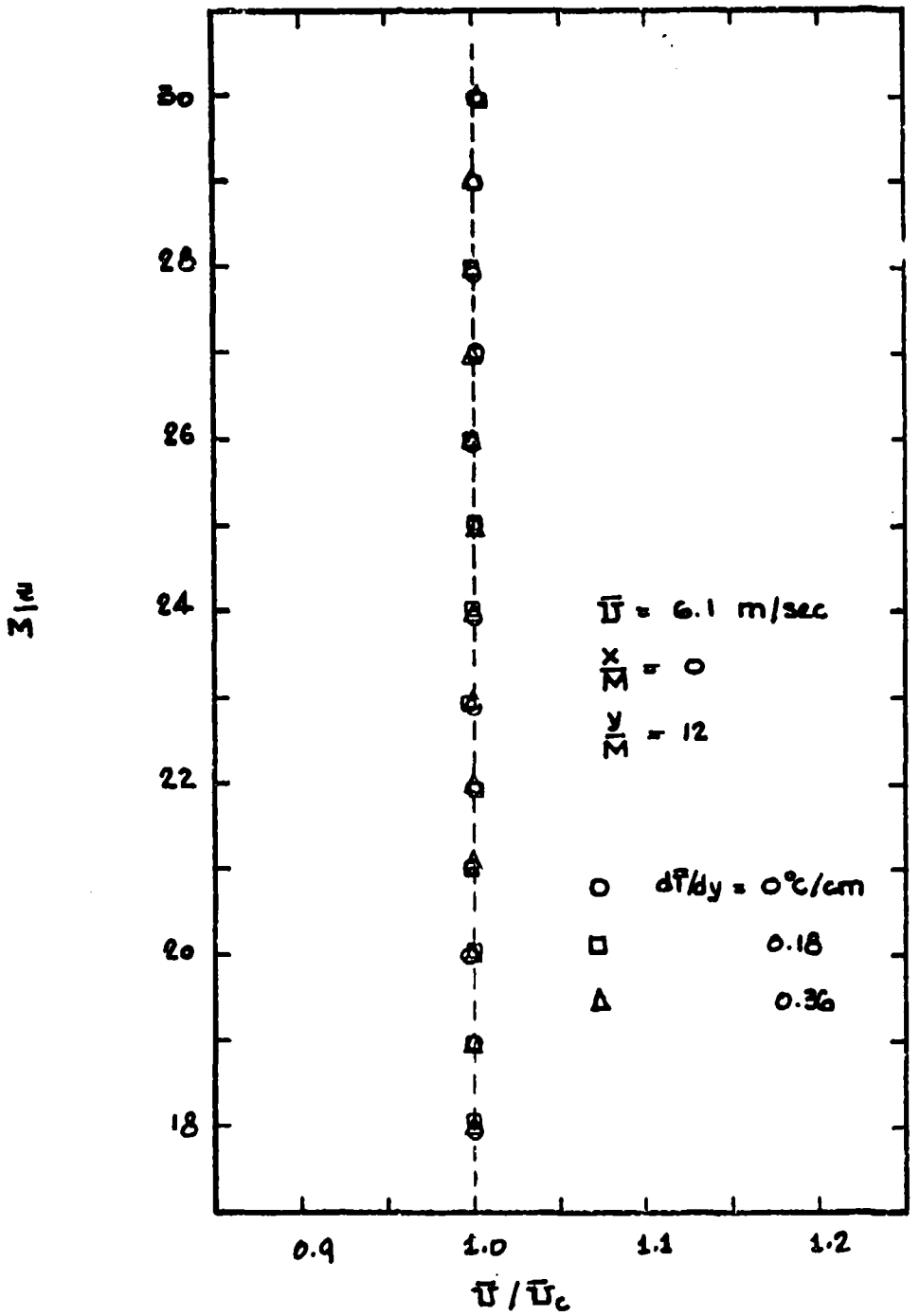


Fig. 22. Temperature effect upon lateral mean velocity distribution

temperature anemometer (55 D05) was used with a DISA 55A25 probe having a 5 micron, platinum plated tungsten wire. A Ball' ,tein R.M.S. meter was used in this connection. A value of 0.07 per cent was found. The best wind tunnels have lower values but in view of the method of heating this background turbulence level was considered satisfactory. The temperature fluctuations within the wind tunnel were determined by means of a resistant thermometer. This consisted of a silver-platinum (Wollestan process) wire, soldered to the tips of a hot-wire probe that was operated in the constant current mode. The wire was first etched in a jet of nitric acid through which a small current flowed. The silver was deplated from a wire over a length of about two millimeters and left a platinum filament of this length. This platinum wire had a diameter of one micron and, depending upon its exact length, a resistance of about 400 Ohms. The wire was operated with a current of less than a milliampere and its resistance measured with the potentiometer. The voltage impressed across this temperature sensor was amplified. The D.C. component was read with a high impedance voltmeter. The oscillating component was further amplified with a A.C. amplifier having a frequency response down to two Hertz. This latter amplifier provided a signal from which the temperature fluctuations, R.M.S. values and other information could be gathered. A calibration of a typical resistance thermometer is shown in figure 23. The effect of the temperature gradient on the amount of temperature fluctuations, R.M.S. value is shown in figure 24. The fluctuations at a given point increase with the temperature gradient and there appears to be some growth if the air particles move along the wind tunnel. Data similar to that shown in the last figure is presented in figure 25. One can infer from these results that at any given temperature gradient the temperature fluctuation approach some asymptotic value.

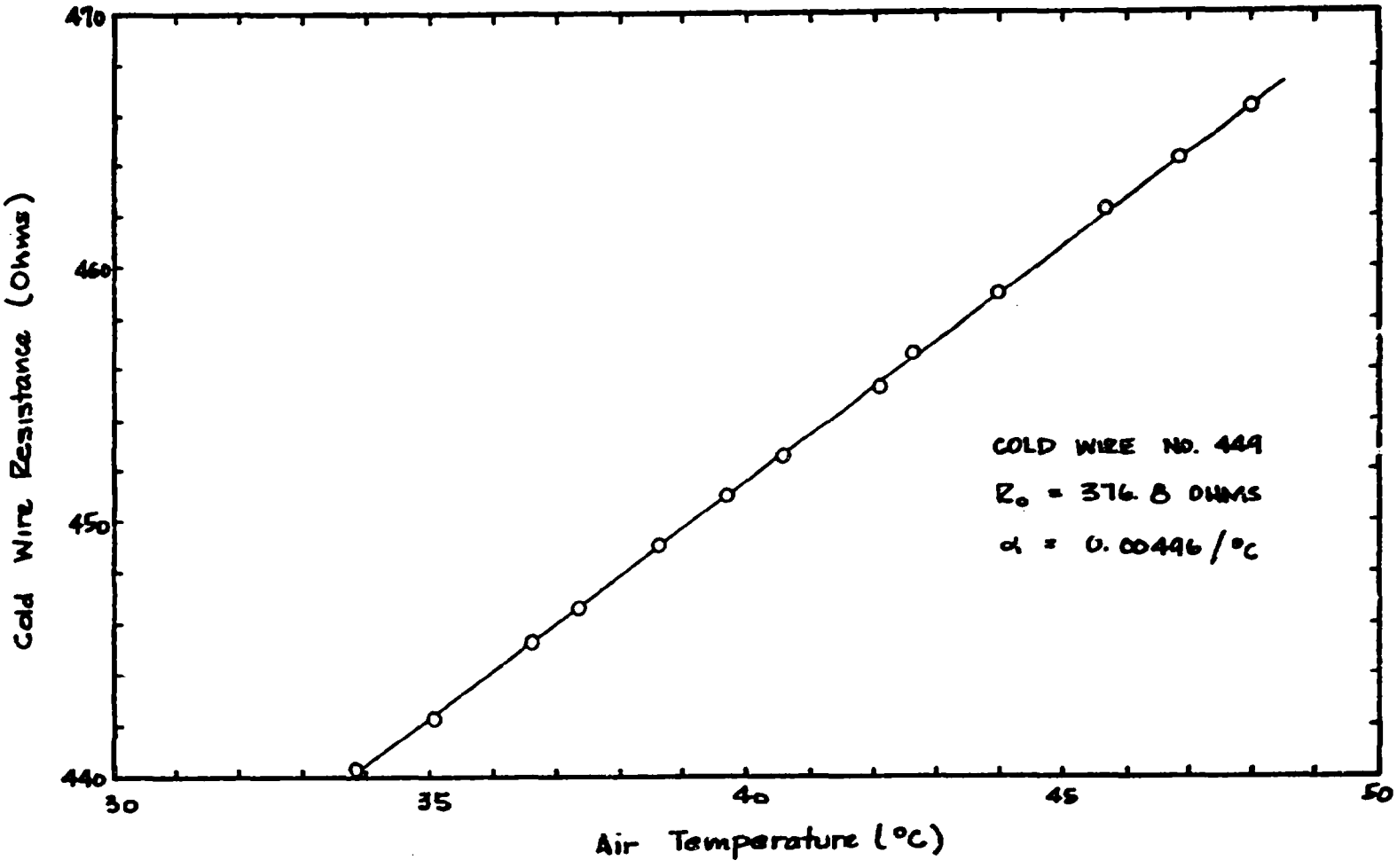


Fig. 23. Typical cold wire calibration

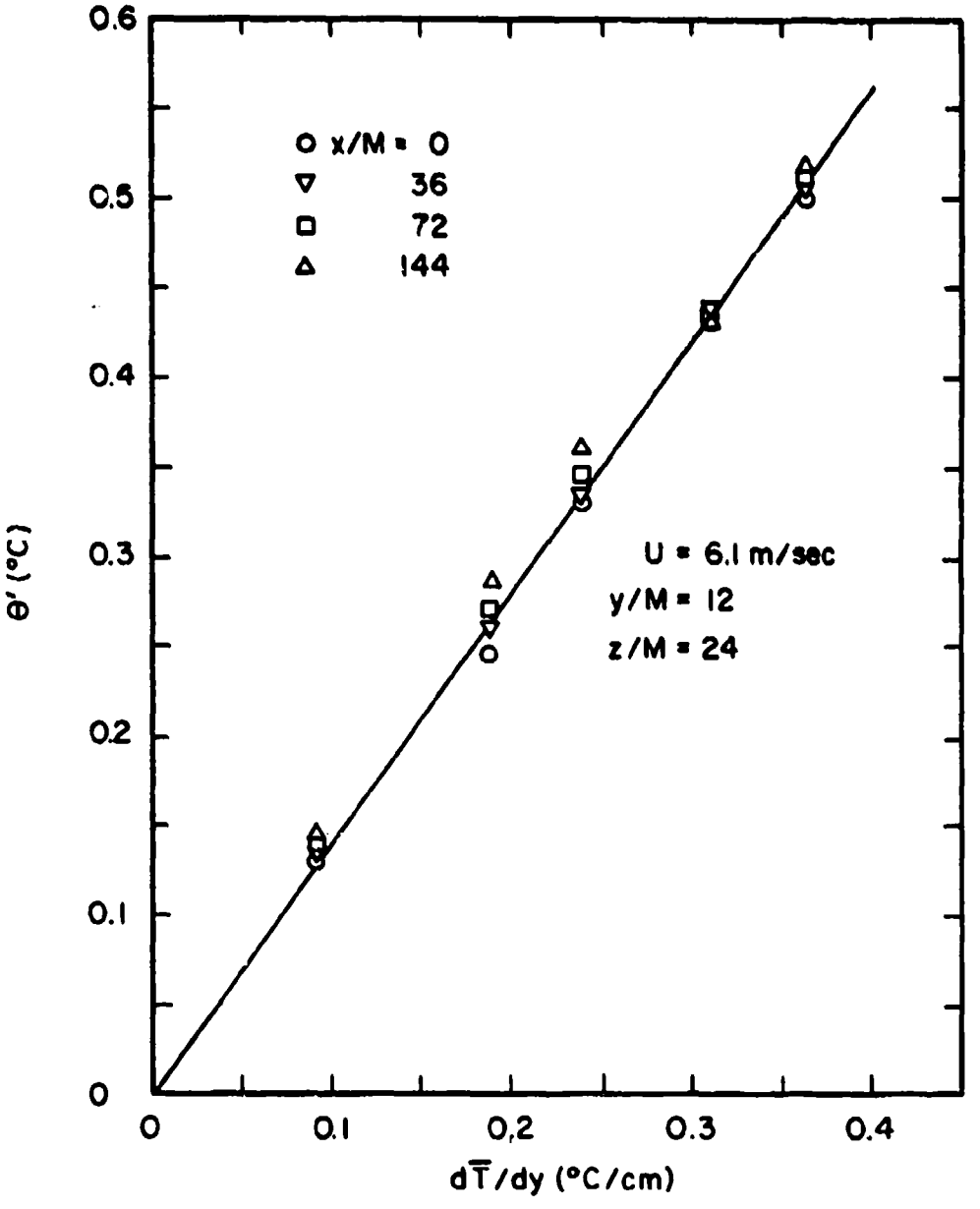


Fig. 24. R.M.S. temperature fluctuation as a function of mean vertical mean temperature gradient

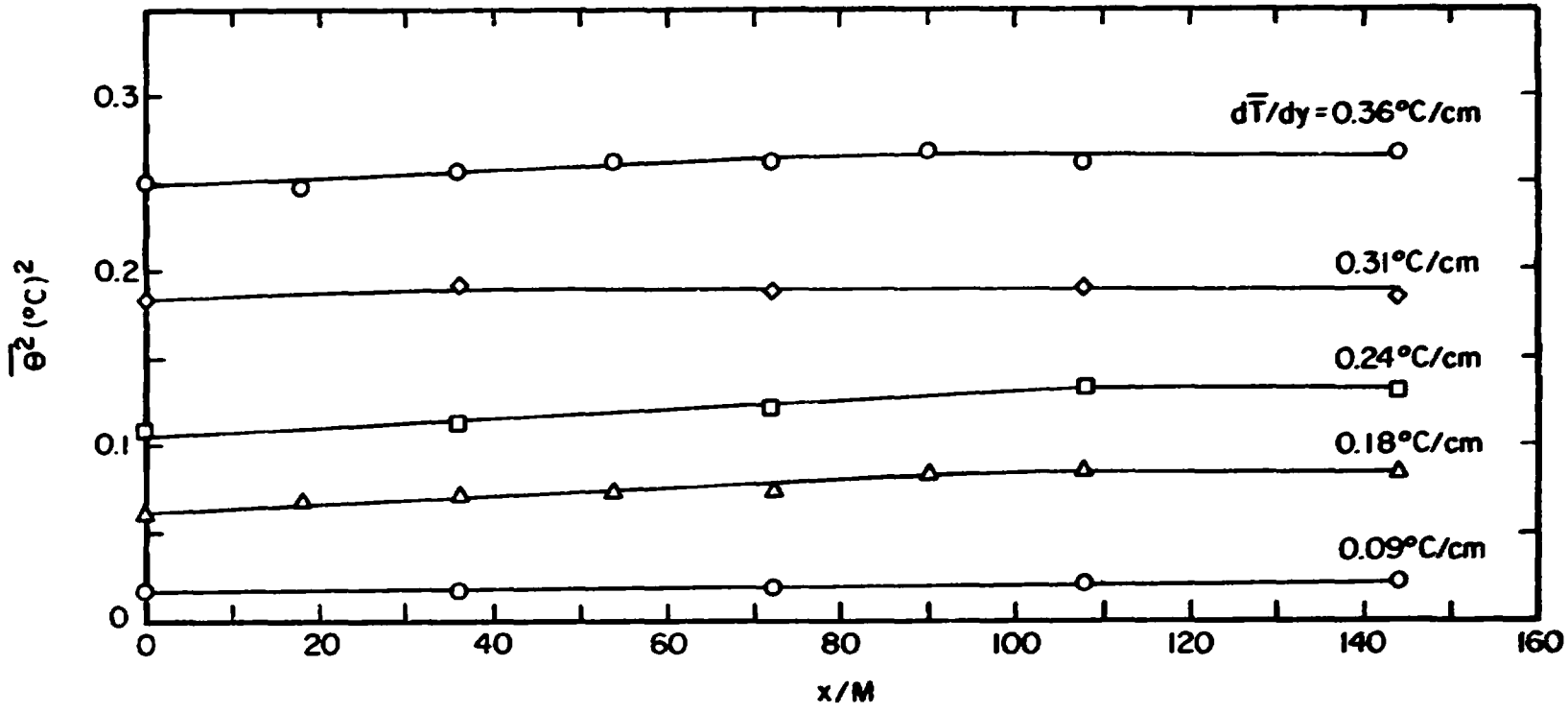


Fig. 25. Growth of temperature fluctuations along wind tunnel centerline (no grid)

## 3. Conclusions

The wind tunnel that was constructed appears to perform exceedingly well over the range of design parameters. The most obvious deficiency is the speed control which under some circumstances caused the tests to be greatly protracted. The velocity and temperature profiles that could be achieved are considered to be good. The background turbulence level is at the upper level of what might be considered a good normal wind tunnel (i.e. without the air heating setter). Temperature fluctuations also appear to be exceedingly minor.

## 4. Acknowlegements

The wind tunnel described in this report was financed largely by funds from the National Science Foundation that were part of Grant No. G-18987 with the University of Michigan. Professor C. S. Yih of this University was the director of that project and had the foresight to propose its construction. Some general design features were specified by Professor L. Garby of the University of Colorado. Mr. James P. Ritz, a graduate student at the time of the building of the facility, was outstanding in all phases of his work. At one stage he overtook complete supervision of the construction while one of the authors was enjoying a postdoctoral fellowship. Many subsequent modifications, including the construction of the third segment of the test section, rebuilding of the heater section as well as the design and construction of the probe manipulators were financed by the Office of Naval Research on Contract N00014-67-A-0181-0008. They also supported the extensive calibration that are described in this report.